IEEE Control Systems Letters paper presented at
2023 62nd IEEE Conference on Decision and Control (CDC)
December 13-15, 2023. Marina Bay Sands, Singapore

Thermodynamic $\mathcal{H}_\infty$ Control of Multidomain Power Networks

Hanz Richter, *Senior Member, IEEE*

***Abstract*— The problem of achieving disturbance attenuation while maximizing energy efficiency in multidomain power networks is considered. Recent results generalizing principles from thermodynamics, in particular those associated with the second law and exergy are used as a basis to define a cost function. A full-information $\mathcal{H}_\infty$ approach is used to guarantee a prescribed level of disturbance attenuation, and a secondary, energy-oriented optimization is carried out over the degree of freedom associated with the non-uniqueness of the $\mathcal{H}_\infty$ solution. The secondary problem is non-convex, requiring a global search. A comprehensive simulation example is included demonstrating the superiority of the optimized controllers, in particular relative to the the central solution of $\mathcal{H}_\infty$ control.**

I. Introduction and Problem Setting

The use of energy-inspired methods *for* control has marked the development of our field since the times of Lyapunov until the successes of passivity-based techniques of the 20th century and beyond. Control *for* energy (e.g., for its efficient management) is a more recent development, and it is receiving renewed attention across many application domains such as energy-aware robotics, microgrids, energy harvesting and more. The first law of thermodynamics (FLT), or energy conservation, provides a common measure of efficiency, η_1, defined as the proportion of work extracted from a process relative to a maximal amount which includes this work and the losses. This measure is immediately applicable to power transfer among systems of any nature: thermal, mechanical, electrical, and so on.

The second law of thermodynamics (SLT) implies that no system may achieve $\eta_1 = 1$ and restricts the direction of heat transfer from hot to cold bodies. In the thermal, fluid and chemical domains, thermodynamic optimization (also known as entropy generation minimization, EGM) is a mature field seeking to reduce the irreversibilities responsible for submaximal efficiency. Some of the methodologies of EGM are indeed optimal control problems [1]. Because the SLT is more restrictive than the FLT, efficiency figures based on the former are more realistic benchmarks of achievable performance than η_1.

Although the SLT is thought to apply to all aspects of the natural world, the macroscopic models used to describe electrical, mechanical and more generally Hamiltonian systems elude a meaningful notion of entropy, a concept central to the SLT. This is because in Hamiltonian systems *instantaneous* power may flow “backwards”, that is, from low- to high-energy subsystems. A formalization of thermodynamics under a dynamical systems approach was undertaken by Haddad and co-workers [2]. The dynamics of interconnected systems which store energy and exchange power with each other and with an external environment are considered without specifying a physical domain, which affords considerable generality. The above restriction on the direction of power flow is adopted on an axiomatic basis, thus excluding lectromechanical power transmission networks and other Hamiltonian systems. Recently, Richter [3] showed that power flow directionality relative to the ordering of energies among subsystems exists for periodic trajectories, using cyclic averages of power and energy rather than instantaneous quantities. The property of *energy cyclo-directionality* (ECD) was introduced and characterized for linear multi-domain power networks using frequency-domain tools.

ECD is the basis for a characterization of power transmission in a broad class of physical systems with concepts and methods borrowed from thermodynamics. In [3], ECD is used to recover results paralleling the SLT and its implications on efficiency. These findings provide a pathway to methodologies to optimize efficiency by means of design parameters or control, as in EGM, but beyond the confines of classical thermodynamics.

This paper explores the effect of control on efficiency under a standard full-information $\mathcal{H}_\infty$ disturbance attenuation approach. The primary control objective is to guarantee a level γ of disturbance attenuation in the $\mathcal{H}_\infty$ sense for the closed-loop mapping disturbances to a performance output. As it is well-known, the solution for a controller meeting this objective is not unique, leaving an unspecified degree of freedom Y, which must be a stable linear transfer matrix of appropriate dimensions such that $||Y||_\infty < \gamma$ [4].

The secondary objective is to improve efficiency by choice of Y, in particular relative to the *central* solution $Y = 0$. An indicator of inefficiency, $\zeta(Y, \omega, w)$, inspired by the SLT and based on the results of [3] is used, which depends on the frequency ω and the disturbance w. A min-max approach is used, where maximization is across disturbance input directions and minimization over a frequency range is done either under a peak criterion or an integral measure.

As observed in the simulation results, the optimal choice of Y may produce *negative* power consumption from the controlled sources, with the load still receiving net power. This corresponds to an enhanced level of power extraction from the disturbances, enabling self-powered operation [5]. Surplus power may even be extracted away from the system and used elsewhere, without detriment to the primary control objective. The results of this paper can thus be interpreted as a method to “make disturbances pay for their own rejection” through the

The author is with the Department of Mechanical Engineering, Cleveland State University, Cleveland, OH 44115, USA h.richter@csuohio.edu. This work was supported by the U.S. National Science Foundation, Grant #200002582

Copyright ©2023 IEEE

optimization of a pertinent efficiency. In contrast to [5], the the benchmark here is the *net* result of energy harvesting from the disturbance and consumption from the controller, which is not required to be passive or realizable with physical components.

II. Energy Cyclo-Directionality and Exergy Efficiency

As in [3], [6], we consider a network $\mathcal{N}$ of n_s subsystems which store energy, exchange power with interconnected subsystems, receive (or return) power to controlled sources and disturbances, dissipate power to the exterior and transfer power to elements external to $\mathcal{N}$, categorized as "loads". Irrespective of subsystem dynamics, it is assumed that an instantaneous power balance holds:

$$\dot{E}_i = S_i - \sigma_i + \sum_{j\in\mathcal{I}, j\neq i} \phi_{ij} - \phi_{Li}, \quad i,j \in \mathcal{I} \tag{1}$$

where $E_i \geq$ are the energies of the subsystems indexed by $\mathcal{I} = \{1, 2, \dots n_s\}$, $\sigma_i \geq 0$ is the power dissipation to the environment, ϕ_{ij} is the net power received by subsystem i from $j \neq i$ and ϕ_{Li} and S_i are the net rate of work performed on the exterior and the net external power supply received, respectively. S_i includes power injected both by control inputs and disturbances. Further, we assume that the subsystems admit periodic trajectories, with well-defined cyclic averages:

Assumption 1: There exist periodic solutions for the quantities in Eq. 1 with period T and frequency $\omega = 2\pi/T$. Furthermore, the quantities $\overline{S}_i = \frac{1}{T}\oint S_i(t)dt$,

$\overline{\sigma}_i = \frac{1}{T}\oint \sigma_i(t)dt$, $\overline{\phi}_{ij} = \frac{1}{T}\oint \phi_{ij}(t)dt$ and $\overline{\phi}_{Li} = \frac{1}{T}\oint \phi_{Li}(t)dt$ exist and are finite. Then the average power balance below holds:

$$0 = \overline{S}_i - \overline{\sigma}_i + \sum_{j=1, j\neq i}^{n_s} \overline{\phi}_{ij} - \overline{\phi}_{Li} \tag{2}$$

Definition 1: [3] $\mathcal{N}$ is said to satisfy energy cyclo-directionality (ECD) if for a periodic solution there exist finite $\gamma_{ij} > 0$ such that

$$\overline{\phi}_{ij}(\overline{E}_i - \gamma_{ij}\overline{E}_j) \leq 0 \tag{3}$$

for all $i, j \in \mathcal{I}$, $i \neq j$.
ECD generalizes the idea of power transmission being directed from high-energy towards low-energy subsystems, which is connected to the SLT [6]. For systems satisfying the passivity condition $\overline{\phi}_{ij} \geq 0$, ECD reduces to finding γ_{ij} satisfying $(\overline{E}_i - \gamma_{ij}\overline{E}_j) \leq 0$. For subsystems with linear time-invariant dynamics, the average energies $\bar{E}_i(v, \omega)$ are quadratic on the inputs v, and it can be shown [3] that a uniform lower bound for γ_{ij} across $\omega > 0$ may be found from

$$\gamma_{ij,crit} = \sup_{\omega>0} \sup_{v\neq 0} \frac{\overline{E}_i(v,\omega)}{\overline{E}_j(v,\omega)} \tag{4}$$

by solving a generalized eigenvalue problem [3].

A. Exergy Efficiency

The following two subsections summarize the findings of [3]. A binary partition $\mathcal{I} = \mathcal{I}_q \cup \mathcal{I}_p$ is used to aggregate the subsystems within $\mathcal{N}$ into just two. This is done to facilitate consideration for port-Hamiltonian systems, which naturally divide energy storage into two generalized kinds: potential and kinetic, indexed respectively with q and p. Thus

$$0 = \delta\overline{Q}_k + \overline{\phi}_{qp} - \overline{\phi}_{Lk} \tag{5}$$

for $k \in \{q, p\}$, where $\delta\overline{Q}_k = \sum_{i\in\mathcal{I}_k}(\overline{S}_i - \overline{\sigma}_i)$, $\overline{\phi}_{Lk} = \sum_{i\in\mathcal{I}_k}\overline{\phi}_{Li}$ and

$$\overline{\phi}_{qp} = \sum_{i\in\mathcal{I}_q}\sum_{j\in\mathcal{I}_p}\overline{\phi}_{ij} = -\sum_{i\in\mathcal{I}_p}\sum_{j\in\mathcal{I}_q}\overline{\phi}_{ij} \tag{6}$$

In classical thermodynamics, entropy $\mathbb{S}$ is defined by

$$d\mathbb{S} = \frac{d\mathbb{U}}{\mathbb{T}} + \frac{d\mathbb{W}}{\mathbb{T}}$$

where $\mathbb{T}$ is the temperature, $\mathbb{U}$ is the internal energy and $\mathbb{W}$ is the work done on the surroundings. Here, a generalized interpretation is made by identifying $E = \mathbb{U}$ and $\phi_L = d\mathbb{W}/dt$ and using shifted and weighted energies instead of temperatures as normalizing denominators. For the periodic averages under consideration we have $\oint dE = 0$ and we define

$$\overline{\mathbb{S}}_r = \frac{\overline{\phi}_{Lq}}{d_q} + \frac{\overline{\phi}_{Lp}}{d_p} \tag{7}$$

where $d_k = c + \beta_k\overline{E_k}$, for arbitrary $c, \beta_k > 0$, $k \in \{q, p\}$. It is straightforward to show [3] that the total average power transferred to the load $\overline{\phi}_L \triangleq \sum\overline{\phi}_{Lk}$ is subject to the upper-bounds

$$\overline{\phi}_L = \overline{\phi}_{Lmax,k} - d_k\overline{\mathcal{X}}_g \leq \overline{\phi}_{Lmax,k}, \quad k = q, p$$

if the *entropy generation rate* $\overline{\mathcal{X}}_g$ is nonnegative:

$$\overline{\mathcal{X}}_g = \frac{\overline{\phi}_{pq}\Delta_{qp}}{(d_q\overline{E}_q + c)(d_p\overline{E}_p + c)} \geq 0 \tag{8}$$

where $\Delta_{qp} = \gamma_e\overline{E}_q - \overline{E}_p$. Clearly, the ECD property ensures $\overline{\mathcal{X}}_g \geq 0$, and in this paper we take $\beta_q = \gamma_e$ and $\beta_p = 1$. The quantity $d_k\overline{\mathcal{X}}_g$ represents the difference between actual and maximal work, and it is referred to as *exergy destruction rate*. An exergy-based efficiency η_2, also known as *SLT efficiency*, is then defined, referenced to the q subsystem:

$$\eta_2 = \frac{\overline{\phi}_{Lq}}{\overline{\phi}_{Lq} + \overline{\phi}_{Lmax,q}} = \frac{1}{1+\zeta}, \quad \zeta = \frac{\overline{\phi}_{pq}\Delta_{qp}}{(\overline{E}_p + c)\overline{\phi}_L} \tag{9}$$

The quantities participating in ζ depend on ω and input directions, and ζ is unaffected by input scaling when $c = 0$.

B. Linear Network Model

$\mathcal{N}$ is an interconnection of sources (including control and disturbance inputs), generalized energy-storing inertial (I) and capacitive (C) elements, dissipative (R) elements and external loads, which may in turn contain elements of these types. Augmented with any dynamics associated with the loads, the augmented network $\mathcal{N}_x$ is assumed to have the state-space representation:

$$\dot{x} = Ax + B_1 w + B_2 u \quad (10)$$

in which $x^T = [q_x^T \quad p_x^T]$ has the generalized displacements q_x of all C-elements and the generalized momenta p_x of all I-elements, with $l \geq 1$ disturbance inputs in vector w and $m \geq 1$ control channels in u. Matrix A is assumed strictly Hurwitz. If the load contains energy-storing elements, the corresponding states are included in x above. However, consistently with Section II, $\overline{E}_p$ and $\overline{E}_q$ correspond to energy storage elements within $\mathcal{N}$ only. The generalized potential and kinetic energies associated with any arbitrary subset of q and p variables assembled in vectors q_n and p_n are given by

$$E_q(q_n) = \frac{1}{2} q_n^T C^{-1} q_n, \text{ and } E_p(p_n) = \frac{1}{2} p_n^T L^{-1} p_n$$

where $C = \text{diag}\{C_i\} \succ 0$ and $L = \text{diag}\{L_i\} \succ 0$ contain the corresponding generalized capacitance and inertia parameters. The average power transmitted to the load, $\overline{\phi}_L$, and $\overline{\phi}_{pq}$ are calculated from corresponding *effort* and *flow* variables e and f, which are outputs of Eq. 10 in the general linear form $Cx + D_1 w + D_2 u$.

III. Cyclic Average Formulas

In Eq. 10, the disturbance and control inputs can be stacked to form input vector $v^T = [w^T \ u^T]$. The generalized momenta and displacements p and q of the energy-storage elements within $\mathcal{N}$ are components of x, thus $p = C_p x$ and $q = C_q x$ for some matrices C_p and C_q. Their Laplace transforms are then

$$P(s) = C_p G_x(s) V(s) \text{ and } Q(s) = C_q G_x(s) V(s)$$

where $G_x(s) = [G_{xw}(s) \ G_{xu}(s)]$, with $G_{xw}(s) = (sI - A)^{-1} B_1$ and $G_{xu}(s) = (sI - A)^{-1} B_2$. For a sinusoidal component of p with amplitude $P_{max,i}$ and frequency ω, the average kinetic energy over one period is given by $\overline{E}_{p,i} = \frac{1}{4L_i} P_{max,i}^2$. Similarly, the average potential energy is $\overline{E}_{q,j} = \frac{1}{4C_j} Q_{max,j}^2$. Summing across all such coordinates, the following formulas give the total average energies:

$$\overline{E}_p(\omega) = \frac{1}{4} V^* M_{po}(\omega) V, \quad \overline{E}_q(\omega) = \frac{1}{4} V^* M_{qo}(\omega) V \quad (11)$$

where the i-th entry of V is the phasor $V_i e^{j\beta_i}$ for V_i real and non-negative and β_i real [7], and

$$M_{po}(\omega) = \widetilde{G}_x(j\omega) C_p^T L^{-1} C_p G_x(j\omega) \quad (12)$$

$$M_{qo}(\omega) = \widetilde{G}_x(j\omega) C_q^T C^{-1} C_q G_x(j\omega) \quad (13)$$

We use $\widetilde{G}$ to denote the adjoint, $G^T(-s)$ and W^* to denote the complex-conjugate transpose of signal $W(s)$ at $s = j\omega$. Dropping frequency dependence from the notation, the weighted energy difference involved in ECD can be written as

$$\Delta_{qp} \triangleq \gamma_e (\overline{E}_q - \frac{1}{\gamma_e} \overline{E}_p) = \frac{\gamma_e}{4} V^* \Delta_o V \quad (14)$$

where $\Delta_o = M_{qo} - \frac{1}{\gamma_e} M_{po}$ The average power exchanged across the p-q interface can be calculated with

$$\overline{\phi}_{pq}(\omega) = \frac{1}{2} \text{Re}\,(e_\phi^* f_\phi) \quad (15)$$

where e_ϕ and f_ϕ are the corresponding effort and flow variables, assumed to be related to the state x by $e_\phi = C_{e\phi} x$ and $f_\phi = C_{f\phi} x$ for some matrices $C_{e\phi}$ and $C_{f\phi}$. It is straightforward to show that

$$\overline{\phi}_{pq}(\omega) = \frac{1}{4} V^* G_{\phi_{pq}}(j\omega) V \quad (16)$$

where $G_{\phi_{pq}} = \widetilde{G}_x (C_{e\phi}^T C_{f\phi} + C_{f\phi}^T C_{e\phi}) G_x$. A similar but longer formula for the average power exchanged with the load can be derived from

$$\overline{\phi}_L(\omega) = \frac{1}{2} \text{Re}\,(e_L^* f_L) = \frac{1}{4} V^* G_{\phi_L}(j\omega) V \quad (17)$$

where the effort and flow variables across the load interface are assumed to be outputs of the form $e_L = C_{eL} x + D_{eL} w$ and $f_L = C_{fL} x + D_{fL} w$.

IV. Full-Information $\mathcal{H}_\infty$ Control

The standard infinite-horizon, full-information control system [4] considers the plant of Eq. 10 and a performance output z of the form

$$z = \begin{bmatrix} Cx \\ Du \end{bmatrix} \quad (18)$$

with the assumptions that (A, B_2) is stabilizable, (C, A) has no unobservable modes on the imaginary axis and $D^T D = I$. Let $R_{zw}(s)$ denote the closed-loop transfer function from the disturbance to the performance output. Then (Theorem 6.3.6 in [4]) the control signal

$$u = -B_2^T P x + Y(w - \gamma^{-2} B_1^T P x) \quad (19)$$

with Y varying in the set of stable linear transfer functions such that $||Y||_\infty < 1$ generates all closed-loop systems such that $||R_{zw}|| < \gamma$ if and only the algebraic Riccati equation

$$PA + A^T P - PFP + C^T C = 0$$

with $F = B_2 B_2^T - \gamma^{-2} B_1 B_1^T$ has a solution $P \geq 0$ such that $A - FP$ is asymptotically stable.

The controller corresponding to $Y = 0$ is designated as the *central* solution. This choice arises from the solution of a secondary optimization problem known as *minimum entropy* $\mathcal{H}_\infty$ control [8]. In this paper we exploit the non-uniqueness of the $\mathcal{H}_\infty$ solution by minimizing a measure having a direct connection to the efficiency of power transmission within and across system boundaries. From Eq. 9, ζ is shown below to be suitable to define an optimization objective. Specifically, either a min-max-max or a min-area-max criterion is used below to obtain an optimization cost from $\zeta(Y, \omega, w)$.

A. Assumptions

The following assumption reflects current knowledge about the ECD property. It is not overly restrictive, as judged from the complexity of the system used in the simulation example and the effectiveness of the optimization. This assumption will be relaxed in future work.

Assumption 2: 1) The boundaries of the p and q subsystems and the load subsystem can be chosen so that all inputs (control and disturbances) enter either the q or the p subsystem only. Without loss of generality, assume that the p subsystem is

the one devoid of inputs. 2) The p and load subsystem are dissipative relative to the supply rates $\phi_{pq} = e_\phi^T f_\phi$ and $\phi_L = e_L^T f_L$, respectively. Further, the load subsystem is assumed to be strictly dissipative.
This assumption implies that the corresponding average powers are non-negative. ECD then reduces to the existence of γ_e such that $\Delta_{qp} \geq 0$ for $\omega \geq 0$ [3]. Also, the load power is strictly positive under this assumption, so that ζ is well-defined and non-negative.

Remark: $M_{po}(\omega)$ are $M_{qo}(\omega)$ are real, symmetric and at least positive semidefinite. If they become singular at some ω, the constant c of Section II-A can be used to shift average energies above zero.

V. Main Results

The following results first ensure that the ECD property is feedback-invariant, that is, it holds as Y is varied. An algorithm based on line searches in a frequency range of interest is presented as a viable solution for low-dimensional problems and used to prove the concept.

Lemma 1: Under the control law of Eq. 19, ζ is given by

$$\zeta(Y,\omega,w) = \frac{W^*\tilde{R}G_{\phi_{pq}}RW}{W^*\tilde{R}G_{\phi_L}RW}\,\frac{W^*\tilde{R}\Delta_o RW}{W^*\tilde{R}M_{po}RW} \tag{20}$$

where

$$R = \begin{bmatrix} I \\ \mathbf{\Phi} \end{bmatrix} \tag{21}$$

with $\mathbf{\Phi} = (I + K_y G_{xu})^{-1}(Y - K_y G_{xw})$, $K_y = K_1 + YK_2$ and $K_1 = B_2^T P$, $K_2 = \gamma^{-2} B_1^T P$. Moreover,

$$X(s) = G_x(s)R(s)W(s) \tag{22}$$

Proof: Consider the open-loop expression for ζ:

$$\zeta(\omega) = \frac{V^*G_{\phi_{pq}}V}{V^*G_{\phi_L}V}\,\frac{V^*\Delta_o V}{V^*M_{po}V}$$

where $V^* = [W^* \; U^*]$. Substitute Eq. 19 into Eq. 10 and take the Laplace transform to solve for the state $X(s)$:

$$X(s) = (I + G_{xu}(s)K_y(s))^{-1}G_x(s)[I \;\; Y^T(s)]^T W(s)$$

Use the above and the well-known MIMO identity

$$K_y(s)(I+G_{xu}(s)K_y(s))^{-1} = (I+K_y(s)G_{xu}(s))^{-1}K_y(s)$$

to find $U(s) = \mathbf{\Phi}(s)$. Then Eq. 20 follows. To show Eq. 22, write $X(s)$ as

$$X(s) = \left[(sI - A)^{-1} + B_2K_y(s))^{-1}(B_1 + B_2Y(s))\right]W(s)$$

Using the same identity and algebraic manipulations, the term in square brackets can be shown to be equal to

$$G_{xw}(s)+G_{xu}(s)(I+K_y(s)G_{xu}(s))^{-1}(Y(s)-K_y(s)G_{xw}(s))$$

which is $G_x(s)R(s)$. That is, closed-loop formulas arise from open-loop expressions by using the feedback transformation $V = RW$. ■

Theorem 1: (Feedback invariance of ECD) The ECD property holds in closed-loop for any Y if it holds in open-loop. Moreover, let the critical constants from Eq. 4 in open- and closed-loop be $\gamma_{e,o}$ and $\gamma_{e,Y}$, respectively. Then $\gamma_{e,o} \geq \gamma_{e,Y}$.

Proof: Let $\mathcal{R}(\omega, v)$ denote the ratio of average energies in Eq. 4. Suppose ECD holds in open-loop and let $V \in \mathbb{C}^{l+m}$. Then there exists $\gamma_{e,o} > 0$ such that

$$\gamma_{e,o} = \sup_\omega \max_{v\neq 0} \mathcal{R}(\omega, v) < \infty$$

Since M_{po} and M_{qo} are Hermitian, the range of $\mathcal{R}$ is a closed interval $\mathcal{I}_\lambda = [\underline{\lambda}(\omega), \overline{\lambda}(\omega)]$ whose ends are the minimum and maximum generalized eigenvalues of (M_{po}, M_{qo}) [9], [10] and

$$\max_{v\neq 0} \mathcal{R}(\omega, v) = \max_{V^*V\leq\kappa^2} \mathcal{R}(\omega, v)$$

for any $\kappa > 0$. Take $\kappa = \overline{\sigma}(R(\omega))$, the maximum singular value of $R(\omega)$ and define the set

$$\beta = \{V \in \mathbb{C}^{l+m} \; : \; 0 < V^*V \leq \kappa^2\}$$

In the closed-loop problem, for each ω we must find $\max_{v\neq 0} \mathcal{R}(\omega, v)$ under the restriction $V = R(\omega)W$, $W \in \mathbb{C}^l$, $w \neq 0$. That is, we consider

$$\max_{w\neq 0} \mathcal{R}(\omega, R(\omega)W) = \max_{0<W^*W\leq 1} \mathcal{R}(\omega, R(\omega)W)$$

The range of $\mathcal{R}(\omega, v)$ under these restrictions is a subset of $\mathcal{I}_\lambda$, which guarantees finiteness of $\sup_\omega \; \mathcal{R}(\omega, v)$, establishing the ECD property in closed-loop. Define the set

$$\beta_R = \{V \in \mathbb{C}^{l+m} \; : \; V = R(\omega)W, W \in \mathbb{C}^l, 0 < W^*W \leq 1\}$$

so that in closed-loop we seek $\gamma_{e,Y} = \sup_\omega \; \max_{v\in\beta_R} \mathcal{R}(\omega, v)$.

To show the inequality, we claim that $\beta_R \subsetneq \beta$. Let $V \in \beta_R$. Then $\exists W$ such that $V = R(\omega)W$ with $0 < W^*W \leq 1$, and

$$V^*V = W^*R^*(\omega)R(\omega)V \leq \overline{\sigma}^2(R(\omega)) = \kappa^2$$

therefore $V \in \beta$ proving the inclusion. Further, $R(\omega)$ is a tall matrix, so dim(col($R(\omega)$)) $\leq l < l + m$. Then we can always pick $\hat{V} \in \mathbb{C}^{l+m}$ such that $\hat{V} \notin$ col $(R(\omega))$ and there is no W such that $\hat{V} = R(\omega)W$. Thus $\hat{v} \notin \beta_R$, proving the claim.

Therefore $\max_{V\in\beta_R} \mathcal{R}(\omega, v) \leq \max_{V\in\beta} \mathcal{R}(\omega, v)$ and taking the supremum over ω proves the desired inequality. ■

Remark: ECD holds with $\gamma_{e,o}$ both in open- and closed-loop. For optimization purposes, however, it is convenient to use the smaller $\gamma_{e,Y}$ corresponding to each candidate Y. A very large γ_e hides the information contained in the Δ_{qp} factor, making optimization less effective.

A. Optimization Problem

At a given frequency ω, $\zeta(Y, \omega, w)$ is the product of two Rayleigh quotients (ratios of positive-definite quadratic functions). A min-max approach is adopted, given that w is uncertain. The inner, maximization problem is to find the worst-case direction of w and the corresponding value of ζ. A separate maximization of each ratio corresponds to a well-known Rayleigh quotient problem [9], [10], with a direct solution given by the eigenvector corresponding to the maximum generalized eigenvalue of the matrices in the numerator and the denominator, as done to find γ_e for ECD. The direction maximizing ζ, however, will generally not coincide with the maximizing eigenvector of either Rayleigh quotient.

This problem is indeed non-convex and NP-hard, and also found in sum-rate maximization for relay networks [11]. These features make it challenging to associate ζ with singular values or system norms. When dimensionality (reflected in m and l) is low, a search across frequencies and input directions is practically feasible and accurate to any desired resolution. This process yields

$$\overline{\zeta}(Y,\omega) = \max_{W^*W\neq 0} \zeta(Y,\omega,w) \quad (23)$$

from which an optimization cost is obtained as described next.

VI. Overview of the Algorithm

At each frequency, maximization over input directions is performed by parameterizing w such that $||w|| = 1$. For w of dimension l, $l-1$ parameters are needed. For $l = 2$, $w^T = [\cos(s) \;\; \sin(s)]$ is taken with $s \in [-\pi, \pi]$ and any desired spacing.

An adaptive feature is included to reduce the width of the interval for s. Since the maximizing w_i at one frequency is expected to remain close to the maximizing direction w_{i-1} at the previous frequency, the interval may be narrowed to a small neighborhood of w_{i-1}. Should s reach either end of this reduced interval, the search can temporarily revert to $[-\pi, \pi]$. This process determines the frequency distribution of the worst-case values of $\zeta(Y,\omega,w)$ over a chosen frequency range $\mathcal{W}$, as in Eq. 23. To obtain a cost, a peak ($\mathcal{H}_\infty$-like) approach may be used, yielding an objective function to be minimized with respect to Y:

$$J_\infty(Y) = \max_{\omega\in\mathcal{W}} \overline{\zeta}(Y,\omega) \quad (24)$$

Alternatively, an integral approach ($\mathcal{H}_2$-like) corresponds to the cost function

$$J_2(Y) = \int_{\omega\in\mathcal{W}} \overline{\zeta}(Y,\omega)d\omega \quad (25)$$

which becomes just a summation due to the finiteness of $\mathcal{W}$. Y of a fixed order may be parameterized, for instance, by including its poles and the zeroes and gains of each $Y(i,j)$, $i \in m$, $j \in l$ in a search vector to be passed to any suitable global optimization algorithm.

VII. Simulation Example

The electromechanical system of Fig. 1 consists of two DC motors $i = 1, 2$ with resistances R_i, inductances L_i and torque constants α_i. Rotational inertias J_i are considered only for the load disks. Viscous damping coefficients b_i and c_i are included for the motor and load, respectively. Two capacitors C_i are connected in parallel with current sources u_i, which are the control inputs. Gear ratios n_i are considered between the motors and the load disks, which are coupled by a torsional spring of constant k. Finally, disturbance torques w_i, shown as τ_{d_i} in the figure act on the motor shafts. A mathematical model is constructed using generalized displacements q and momenta p as components of the state vector x. The model description and parameter values are available through the code accompanying this paper.

Control objectives: The primary objective is to maintain the

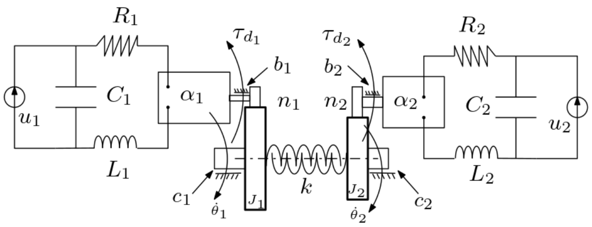

Fig. 1. Twin electromechanical drive used in the simulation example.

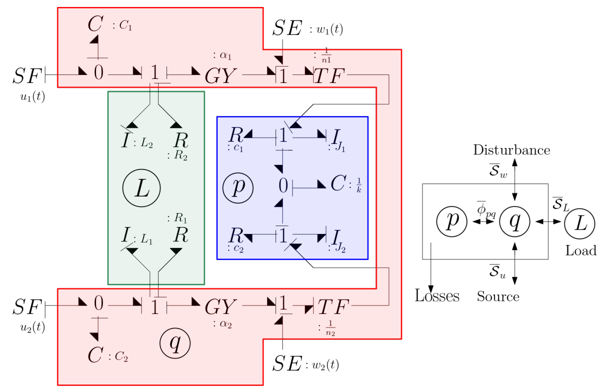

Fig. 2. Bond graph and network connectivity for the twin electromechanical drive of the simulation example.

relative rotation between the disks small in the presence of disturbances (i.e., to limit the torque on the spring to some safe level) while penalizing excessive control currents. This objective is addressed by using $q_L = \theta_1 - \theta_2$ in the performance output $z^T = [\rho q_L \;\; D^T u^T]$. $D = I$ was taken and the results below follow from choosing $\rho = 10$.

The secondary objective is to maximize the power transmitted to the load while extracting the most power from the disturbances, so that the power consumption from the controlled sources is reduced. In this example the average power transmitted to the load corresponds to viscous friction on the load shafts and it can be interpreted as "useful" work (this friction could arise, for example, from stirring a viscous liquid in some production process). Whenever the power consumption from the sources is negative, "self-powered" operation has been achieved with a system which also complies with a primary regulation objective. In this case, the surplus power could be extracted, for instance by tapping current from the capacitors.

A bond graph representation (Fig. 2) is a good visualization of power flows and the distribution of energy storage, dissipation and conversion elements. Through its causal notation, it also provides information about the structure of the system's dynamics [12]. Figure 2 also defines the boundaries of the p, q and load subsystems and the connectivity of the power network. The p subsystem and the load are dissipative, while the controlled sources and the disturbances are connected to the q subsystem only. These features meet Assumption 2. Moreover, only the q subsystem is connected to an external load (this is incidental but not required).

The primary suboptimal $\mathcal{H}_\infty$ was solved using the standard Riccati equation method [4] with performance levels γ

reduced by iteration. A near-optimal value of γ was selected and the corresponding feedback gains K_1 and K_2 calculated. For the secondary objective, a search among Y of second order with $m = 2$ inputs and $l = 2$ outputs was conducted. Two zeroes and one gain for each entry, along with two poles of U make for 14 search parameters. Upper and lower bounds were placed to limit the gains, the bandwidth and to ensure left-half plane poles. A log-spaced set $\mathcal{W}$ of 100 frequencies between 0.1 and 100 rad/s is used in the algorithm compute $\overline{\zeta}$ for Y candidates, normalizing by $||Y||_\infty$. The maximization over input directions w was done by a line search with $w = [\cos(s)\ \ \sin(s)]^T$ for $s \in [-\pi,\ \pi]$ with a spacing of 0.05 rad. The adaptive feature considerably reduces the width of this interval and results in a faster search.

The problem was solved using J_∞ and again using J_2. The optimizer computes $\gamma_{e,crit}$ for each candidate Y instead of using the larger, open-loop value that guarantees ECD for any Y (Theorem 1). Matlab's `patternsearch` was found to be very efficient in finding the solutions. Their corresponding $\gamma_{e,crit}$ were found to be very close to each other and to the value corresponding to $Y = 0$. The largest value was used to evaluate all three solutions uniformly. Figure 3 shows the magnitude of $\overline{\zeta}$ (arbitrarily scaled) for the central and optimized controllers. The optimized solutions are seen to be most effective below certain frequency. The two solutions offer similar worst-case performances, however their parameters are very different, as it could be shown by plotting the singular values of Y.

Discussion: Table I shows a balance of average power for each solution as determined by a time-domain simulation in two cases: first, for $\omega = 1$ rad/s and sinusoidal disturbances, each controller was tested with its respective worst-case input direction (amplitude ratio). Separately, white noises past low-pass filters with cutoff frequencies of 1 rad/s were applied to each channel in w. The total power input $\overline{S}_q$ in Eq. 2 was split into contributions from the control input, $\overline{S}_u$, and the disturbance $\overline{S}_w$.

The FLT efficiencies $\eta_1 = \overline{\phi}_L/\overline{S}_q$ are, as expected, very low when the worst-case directions corresponding to each Y are used. The optimized solutions, however, have higher η_1 and extract a large amount of power from the disturbances, allowing them to return power to the source, making self-powered operation feasible. With the noise input, disturbances appear in all directions, and the central controller is more efficient under the η_1 criterion.

The FLT may not the best criterion to evaluate the results, since it does not consider the benefit of "selling" the surplus power. An economics-oriented *extraction efficiency* is a more sensible measure:

$$\eta_x \triangleq \frac{\overline{\phi}_L - \overline{S}_u}{\overline{S}_w} = 1 - \frac{\Sigma\, \overline{\sigma}_i}{\overline{S}_w} \tag{26}$$

The numerator of the definition contains the net utility and the denominator the available resource. When the losses exceed the power extracted from the disturbances (as in the first row of the table), the utility is negative. The upper limit to η_x is 1. Table I shows a remarkable superiority of the optimized controllers relative to this measure. The results also shows that the approach introduced here is not equivalent to plain minimization of losses or maximization of η_1.

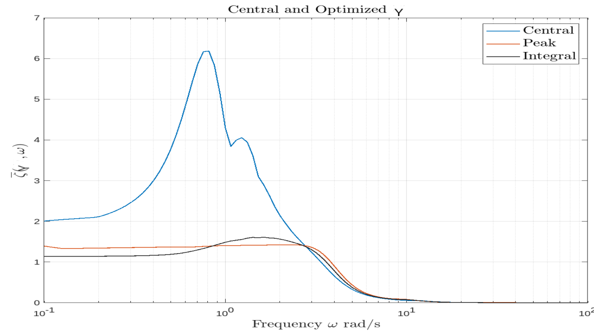

Fig. 3. Worst-case ζ for the optimized and central controllers

Worst-case	$\overline{S}_u$	$\overline{S}_w$	$\overline{\sigma}$	$\overline{S}_L$	$\eta_1(\%)$	$\eta_x(\%)$
Central	24.5	10.9	34.8	0.57	1.56	< 0
Peak-optimized	-67.0	285.9	210.2	8.30	3.8	26.3
Area-optimized	-29.0	165.6	130.7	5.50	4.1	20.8
White noise	$\overline{S}_u$	$\overline{S}_w$	$\overline{\sigma}$	$\overline{S}_L$	$\eta_1(\%)$	$\eta_x(\%)$
Central	-6.20	99.7	58.0	35.3	37.78	41.65
Peak-optimized	-21.9	77.0	49.7	5.30	9.61	35.37
Area-optimized	-22.5	89.0	50.7	15.7	23.54	42.85

TABLE I

TIME-DOMAIN SIMULATION RESULTS AT $\omega = 1$ RAD/S AND WITH A LOW-PASS FILTERED WHITE NOISE. POWER IS SHOWN IN MILLIWATTS.

REFERENCES

[1] K.-Y. Teh and C. F. Edwards, "An Optimal Control Approach to Minimizing Entropy Generation in an Adiabatic Internal Combustion Engine," *Journal of Dynamic Systems, Measurement, and Control*, vol. 130, no. 4, 06 2008.

[2] W. M. Haddad, *A Dynamical Systems Theory of Thermodynamics*. Princeton University Press, 2019.

[3] H. Richter, "Energy cyclo-directionality, average equipartition and exergy efficiency of multidomain power networks," *IEEE Control Systems Letters*, vol. 6, pp. 3337–3342, 2022.

[4] M. Green and D. Limebeer, *Linear Robust Control*. Prentice-Hall, 1995.

[5] C. Ligeikis and J. Scruggs, "An LQG-inspired framework for self-powered feedback control," in *IEEE Conference on Decision and Control*, 2022, pp. 4519–4526.

[6] W. Haddad, V. Chellaboina, and S. Nersesov, *Thermodynamics: A Dynamical Systems Approach*. Princeton Series in Applied Mathematics, 2005.

[7] S. Skogestad and I. Postlethwaite, *Multivariable Feedback Control*. Wiley, 1996.

[8] D. Mustafa and K. Glover, *Minimum-Entropy $\mathcal{H}_\infty$ Control*, ser. Lecture Notes in Control and Information Sciences, M. Thoma and A. Wyner, Eds. Springer, 1990.

[9] S. Boyd and L. Vandenberghe, *Convex Optimization*. Cambridge: Cambridge University Press, 2004.

[10] G. Golub and C. van Loan, *Matrix Computations*. Baltimore and London: Johns Hopkins University Press, 1996.

[11] J. Zhang *et al.*, "Sum rate maximization for multi-pair two-way relaying with single-antenna amplify and forward relays," in *2012 IEEE International Conference on Acoustics, Speech and Signal Processing (ICASSP)*, 2012, pp. 2477–2480.

[12] D. C. Karnopp, D. L. Margolis, and R. C. Rosenberg, *System Dynamics: Modeling, Simulation, and Control of Mechatronic Systems*. John Wiley & Sons, 2012.